MAGNETIC Fe_3O_4@SiO_2-Pt AND Fe_3O_4@SiO_2-Pt@SiO_2 STRUCTURES FOR HDN OF INDOLE.

Robinson Dinamarca[ad], Verónica Valles[b*], Brenda Ledesma[b], Cristian Campos[a], Gina Pecchi[ac], Andrea Beltramone [b*]

[a] *Fac. Ciencias Químicas. Universidad de Concepción, Concepción, Chile.*

[b]*Centro de Investigación en Nanociencia y Nanotecnología (NANOTEC), Facultad Regional Córdoba, Universidad Tecnológica Nacional, Maestro López y Cruz Roja Argentina, 5016, Córdoba, Argentina;*

[c] *Millenium Nuclei on Catalytic Processes towards Sustainable Chemistry (CSC), Chile.*

[d] *Facultad de Educación. Universidad de Concepción, Chile.*

**E-mail:vvalles@frc.unt.edu.ar*

Resumen

Se informa el efecto de una segunda cubierta porosa de SiO_2 en la actividad y selectividad del catalizador Fe_3O_4@SiO_2-Pt en la hidrodenitrogenación de indol. La doble estructura de Fe_3O_4@SiO_2-Pt se preparó recubriendo nanopartículas de Fe_3O_4 con TEOS y una impregnación adicional de 1,0% en peso de Pt en la estructura de Fe_3O_4@SiO_2 funcionalizada con (3-aminopropilo)trietoxisilano. La segunda cubierta porosa de SiO_2, obtenida utilizando la plantilla CTAB, con una distribución de tamaño de poro estrecha y bien definida, cubrió el catalizador Fe_3O_4@SiO_2-Pt. La caracterización completa por TEM, ICP-OES, XRD, isoterma de adsorción de N_2 a 77 K y VSM de los catalizadores indica estructuras homogéneas core@shell con un nano tamaño controlado de Pt metálico. Se demostró un efecto significativo de la doble capa de SiO_2 en el rendimiento catalítico tanto por una mayor actividad para eliminar el átomo de nitrógeno de la molécula de indol, presente en el combustible líquido modelo, como por la mejora de la estabilidad catalítica, lo cual se observa en la obtención de cuatro ciclos de reacción consecutivos con solo una ligera disminución en la conversión.

Palabras clave: core@shell, platino, materiales mesoporosos, Indol, HDN.

Abstract

The effect of a second porous SiO_2 shell in the activity and selectivity of the Fe_3O_4@SiO_2-Pt catalyst in the hydrodenitrogenation of indole is reported. The double Fe_3O_4@SiO_2-Pt@SiO_2 structure was prepared by coating Fe_3O_4 nanoparticles with TEOS with a further impregnation of 1.0 wt.% of Pt on the (3-aminopropyl)triethoxysilane functionalized Fe_3O_4@SiO_2 structures. The second porous SiO_2 shell, obtained by using CTAB template, covered the Fe_3O_4@SiO_2-Pt catalyst with a well-defined and narrow pore sized distribution. The fully characterization by TEM, ICP-OES, XRD, N_2 adsorption isotherm at 77 K and VSM of the catalysts indicates homogeneous core@shell structures with a controlled nano-size of metallic Pt. A significant effect of the double SiO_2 shell in the catalytic performance was demonstrated by both a higher activity to eliminate the nitrogen atom of indole molecule present in model liquid fuel and the improvement of the catalytic stability reaching four consecutive reaction cycles with only a slight conversion level decrease.

Keywords: core@shell, platinum, mesoporous materials, indole, HDN.

Los autores están de acuerdo en incluir el presente trabajo en un volumen especial dedicado al CICAT 2020 en alguna de las revistas internacionales: Catalysis Today o Topics in Catalysis en caso de que los revisores y el comité científico así lo designe.

1. Introduction

The presence of polyaromatic and cyclic compounds in diesel negatively affects the environment and reduce the quality of diesel, as well as lowers the cetane number, which is indicative of the ease of ignition thereof. Hydrotreatment, witch includes multiple reactions, is one of the most efficient method for the removal of N and S, from refinery currents, as well as for the saturation of alkenes and aromatics [1-4]. The HDS has been extensively studied because sulfur is a pollutant that is present in higher proportions in crude oils of lower quality and also as an important catalyst deactivator because of poisoning. However, removal of nitrogen is harder than sulfur removal, which leads to the importance of the study of the HDN reaction [4-8]. In this process of heterogeneous catalysis, the industry currently uses variations of the following combinations Co(Ni)Mo(W)/Al2O3. Our previous works have shown that the acid support, the formation of bimetallic alloys and the introduction of heteroatoms can greatly improve the performance of deposited metals as active phase [3,7-10]. Likewise, the supports with large surface areas have been very studied since they allow to achieve a great dispersion of the active phase, significantly improving the yield of the reactions [7-11].Among the challenges that arise in the development of catalysts for the refining of crude oil, the factors associated with their reuse are decisive, both the characteristics that allow the separation of the catalyst from the reaction medium, as well as its recovery and the degree of activity that can be maintained in multiple reaction cycles. Accordingly, other interesting catalysts are core-shell nanoparticles (CSNs), designated as core@shell, that are formed with nuclei (inner materials) and shells (external material) at nanoscale. Silica-based CSNs have been extensively studied because silica is considered inert, a simple dispersant of the active phase, although can react with metal precursors to form silicates of Ni, Co, Cu, Zn and Ce with different reactivity [12-15]. Core@shell silica microspheres with ultra-small encapsulated nanoparticles of Pd have been highlighted as efficient and easily recyclable for the catalytic hydrogenation of various groups of olefins, alkynes, keto and nitro groups [16, 17]. Schätz et al. [18] in their review article, made an extensive analysis of various catalyst supported and their properties for magnetic separation. The application of core@shell silica microspheres, with ultra-small encapsulated nanoparticles of Pt, in the catalytic hydrotreatment process was not found in literature. The main objetive of this work is to develope homogeneous core@shell structures with a controlled nano-size of metallic Pt and study the effect of the double SiO_2 shell in the catalytic performance in the HDN of indole.

2. Materials and Methods

2.1- Synthesis

The Fe_3O_4 NPs were synthesized by a solvothermal method following Long et al. [19], FeCl3 (Merck®) was dissolved in a polyvinyl pyrrolidone (PVP K30, Sigma®) solution in ethylene glycol (EG, Merck®) and sodium acetate as nucleating agent. The mixture was transferred to a Teflon autoclave and isothermally treated at 200°C for 8 h. The solid obtained was separated by magnetization and washed several times with absolute ethanol. The Fe3O4-core NPs were coated with SiO2 using the Stöber method [19]. Fe3O4 NPs were dispersed in a mixture of ethanol, water and ammonia, after that tetraethyl orthosilicate (TEOS, Merck®) was slowly added to the dispersion under stirring for 6 h. The Fe3O4@SiO2 solid was separated by magnetization and washed several times with an ethanol-water mixture. In order to promote an active Pt immobilization and dispersion on the surface of the material, the surface of the Fe3O4@SiO2 was functionalized with (3-aminopropyl)trimethoxysilane (AMPTS, Merck®, 1 mLg-1 of solid), a coupling agent refluxing in toluene for 24 h under mechanical stirring. The solid was separated by magnetization, washed with a toluene-acetone mixture, and dried in oven at 50°C for 12 h. The functionalized material was dispersed in a K2PtCl6 (Merck®) solution with an amount of precursor necessary to produce 1.0 wt% systems with respect to Fe3O4@SiO2. The material was placed in contact with the solution for 3 h under mechanical stirring and then reduced with a fresh solution of NaBH4 (Merck®). The second coating of SiO2 was deposited on the Fe3O4@SiO2-Pt surface by a modified Stöber method reported previously [20] using TEOS as a precursor, triethanolamine (TEA) as a basic catalyst and hexadecyltrimethylammonium bromide (CTAB, Sigma®) as stabilized and soft template. Finally, the CTAB template was removed by ion exchange using ammonium nitrate in ethanol dissolution under reflux conditions, obtaining the Fe3O4@SiO2-Pt@mSiO2 material.

2.2-Characterization

The morphology and microanalysis of the structures were studied by scanning transmission electron microscopy with energy dispersive X-ray spectroscopy (STEM-EDS) using an FEI Tecnai ST F20 microscope (FEI, Hillsboro, OR, USA) operating at 200 kV. Adsorption isotherms were obtained at 77 K in a Micromeritics ASAP 2010 instrument (Norcross, GA, U.S.A). X-ray powder diffraction profiles were obtained in a Rigaku Diffractometer with Cu Kα radiation (λ = 1.5418 Å) and a nickel filter (Rigaku, Tokyo, Japan). The magnetic behavior was studied using a Lakeshore series 7400 vibrating sample magnetometer (VSM) in an applied field of 20 kOe at 27 °C (Lakeshore, New Orleans, LA, USA). Pt and Fe contents were determined by inductively coupled plasma - optical emission spectroscopy (ICP-OES) with a Perkin-Elmer Optima 2100 DV instrument (Perkin Elmer, Waltham, MA, USA). The catalyst contents were determined after digestion in a 1:3 mixture of HNO3:HCl. XPS was obtained on a STAIB Instruments brand RQ-300 X-ray Source spectrophotometer (XPS RQ300/2, StaibInstrumente GmbH, Langenbach, Germany). The monochromatic radiation used as an excitation source is that of Al Kα (hν = 11486.6 eV) operated at 75W.

2.3-Catalytic activity

The hydrodenitrogenation reactions of indole were carried out at 250 °C and 15 atm of H2 and 500 rpm in a 600 mL stirred autoclave (Parr Pressure Reactor 4536, Parr Instrument Company, Illinois, USA). The typical procedure was as follows: 150 ppm of N as indole was dissolved in 50 mL of dodecane (0.01 mol L-1). The mixture was placed into the autoclave and the catalyst (250 mg) was transferred to the reactor. The reaction time was 8 h; samples were taken every hour. The products were analyzed with a HP 5890 Series II GC and HP-5 capillary column and identified by GC/MS.

3. Results and Discussion

3.1-Characterization

Figure 1 presents the high-resolution transmission electron microscopy (HR-TEM) for the image sequence obtained at each step of the catalyst synthesis; the Fe3O4-core image is shown in Figure 1.a. Figure 1.b reveals the CSNs where the Fe3O4 core is covered by a layer of SiO2 close to 45 nm thick (Table 1). In Figure 1.c and Figure 1.d it can be seen a successfully impregnation-reduction process obtaining Fe3O4@SiO2–Pt and Fe3O4@SiO2–Pt@mSiO2 catalysts, respectively. Both catalysts present similar Pt size distribution and an average particle size of 3.5 nm (Table 1). The SiO2 coating generated by the Stöber method did not modify the distribution or increase the average size of the Pt-NPs on the surface of the material. The micrographs show the formation of an uniform coating on the surface of both catalysts, with channels perpendicular to the surface that correspond to the porosity of the material formed during the removal of the organic CTAB template used as porosity directing agent. It is noticeable the preferential alignment of the surfactant and the silica oligomer with the core@shell in the performed structures.

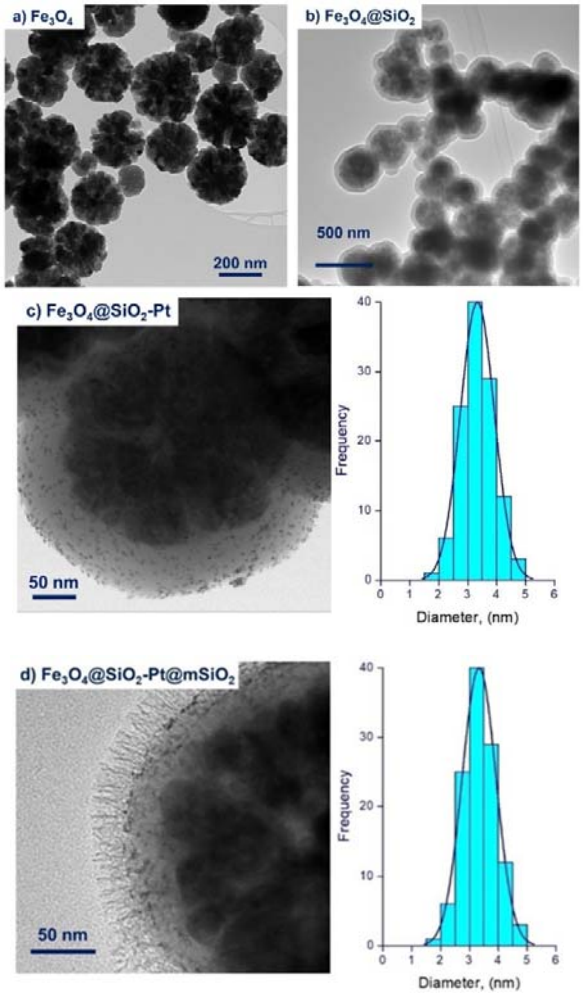

Figure 1. HR-TEM of the synthesized Fe_3O_4-NPs and core@shell structures.

The catalysts were characterized by ICP-OES to determine the Pt content, as summarized in Table 1. The Fe3O4@SiO2–Pt catalyst contains slight lower Pt than the nominal value, while for the

Fe3O4@SiO2–Pt@mSiO2 catalysts the Pt loading is largely lower than the nominal. The larger difference in the Pt content for Fe3O4@SiO2–Pt@mSiO2 is attributed to the second mSiO2 shell of core@shell particles and not due to the leaching effect. When the mesoporous SiO2 shell is coated around the Fe3O4@SiO2–Pt structures, a uniform increase in the size of the second shell is observed reaching 51 nm of thickness mean diameter (see Table 1). The increase of the thickness provides a dilution of the Pt active phase compared to the Fe3O4@SiO2–Pt structures, in the same way of the increase of the SiO2 shell thickness.

Table 1. HR-TEM characterization, ICP-OES, S_{BET} and Pt $4f_{7/2}$ binding energy.

	Fe_3O_4@ SiO_2-Pt	**Fe_3O_4@SiO_2-Pt@mSiO_2**
Core Mean Diameter (nm)	229±75	231±42
Thickness SiO_2 Mean Diameter (nm)	45 ± 12	96 ± 15 (51 ± 14)[1]
Pt Mean Diameter (nm)	3.6 ± 1.0	3.4 ± 0.8
Pt Content (%)	0.7 (1.0)[2]	0.35 (1.0)[2]
S_{BET}(m^2g^{-1})	11	178
Pt $4f_{7/2}$(eV)	70.9	--

[1] Second shell thickness SiO_2 mean diameter in brackets; [2] nominal value in brackets.

Figure 2 illustrates the XRD patterns of the synthesized materials. All systems show the diffraction peaks characteristic of magnetite, Fe3O4 (JCPDS 19-0629) [21]. The Fe3O4 phase was not modified during the SiO2 coating. This finding indicates that the crystalline phase of the material is restricted to the magnetite core. Only for the Fe3O4@SiO2–Pt a diffraction peak at 2θ = 39° is detected, corresponding to the surface metallic Pt (JCPDS 04-0802). The low intensity of this signal is attributed to the average particle size of the Pt clusters below the detection limit of the XRD technique. The high dispersion of the Pt crystalline phase is in line with the homogenous distribution of Pt -NPs on the surface of the SiO2 shell observed by HR-TEM and the surface XPS technique confirms the presence of metallic Pt (see below).

Figure 3 shows the spectra of Pt $4f_{7/2}$ for Fe_3O_4@SiO_2-Pt catalyst, with BE of 70.9 eV attributed to the metallic Pt species. Surface metallic Pt was not detected in the system with the second SiO_2 coating, this was attributed to the coverage with the second shell. Table 1 presents the results obtained for S_{BET} calculated from the N_2 adsorption-desorption isotherms at 77 K shown in Figure 4.

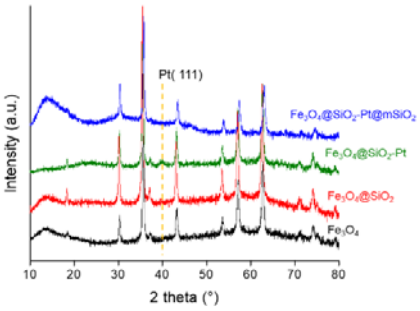

Figure 2. XRD of the synthesized Fe_3O_4-NPs and core@shell structures.

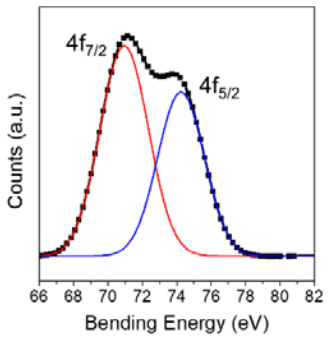

Figure 3. XPS of the Pt $4f_{7/2}$ of Fe_3O_4@SiO_2-Pt core@shell structure.

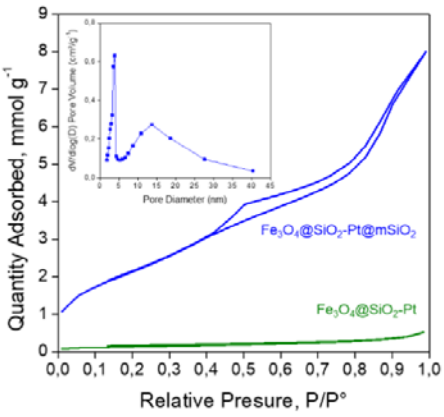

Figure 4. N_2 adsorption isotherms and pore size distribution of the core@shell structures.

The Fe_3O_4@SiO_2–Pt shows an isotherm typical of type II materials and S_{BET} value of 11 m^2g^{-1}. After the deposition of the second shell the isotherm changes to mesoporous type IV materials with a large increase in the specific area. The hysteresis loop instead of cycle for

Fe_3O_4@SiO_2-Pt@mSiO_2 corresponds to type H3 pores type parallel plates according to the IUPAC classification [22]. The pore size distribution shows a bimodal distribution with a narrow distribution centered at 3.8 nm and a wider distribution centred at 10 nm associated with the interstitial spaces of the aggregates of the particles. The narrow distribution of mesopores at 3.8 nm is attributed to the removed CTAB organic template.

Fe_3O_4@SiO_2–Pt and Fe_3O_4@SiO_2–Pt@mSiO_2 materials exhibit the ferromagnetic properties of the started Fe_3O_4–NPs as it can be seen in Figure 5. The magnetic saturation (M_s) value of the Fe_3O_4–NPs changes with subsequent coverage, due to the relative decrease of Fe_3O_4 content respect to the presence of the SiO_2 shell. The Fe_3O_4 core corresponds to magnetization curves with absence of a hysteresis cycle, characteristic of superparamagnetic materials. The decrease of the M_s of 91 $emug^{-1}$ for magnetite phase (Fe_3O_4) to 45 emu g^{-1} for Fe_3O_4@SiO_2-Pt and 25 emu g^{-1} for Fe_3O_4@SiO_2-Pt@mSiO_2 is as result of the effect of the coating with SiO_2. Even though, the relative lower value of M_s, between 25 to 45 $emug^{-1}$ was enough for the efficiently removal below 1 min of the micro-sized particles, and reflected the ability of these catalysts to respond to an external magnetic field. That allows to be quickly separated from the liquid phase [23].

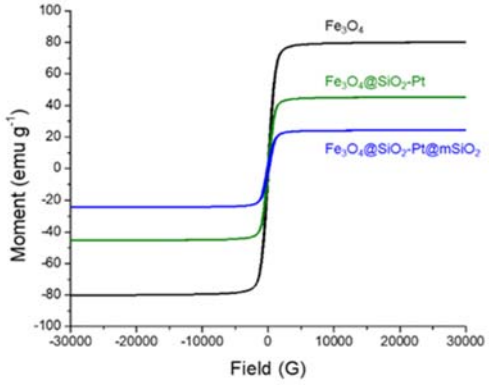

Figure 5. VSM of the synthesized Fe_3O_4-NPs and core@shell structures.

3.2-Catalytic activity

The reaction network of the hydrodenitrogenation of indole proposed by Zhang and Ozkan is shown in Scheme 1 [24]. According this pathway, ECH and EB are the two main products from HDN of indole. The only identified products, after the experiments performed in this work, were indoline (HIN), o-ethylaniline (OEA), ethylbenzene (EB) and ethylcyclohexane (ECH); these accounted for almost 95% of the total products.

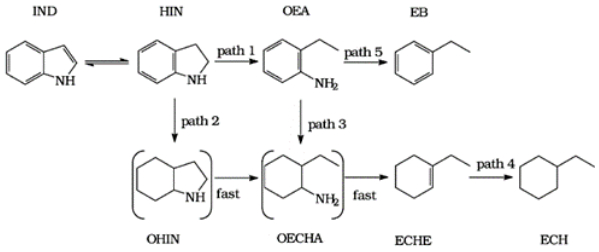

Scheme 1. Reaction pathways for HDN of indole: indole (IND), indoline (HIN), o-ethylaniline (OEA), ethylbenzene (EB), octahydroindole (OHIN), o-ethylcyclohexylamine (OECHA), ethylcyclohexene (ECHE), ethylcyclohexane (ECH).

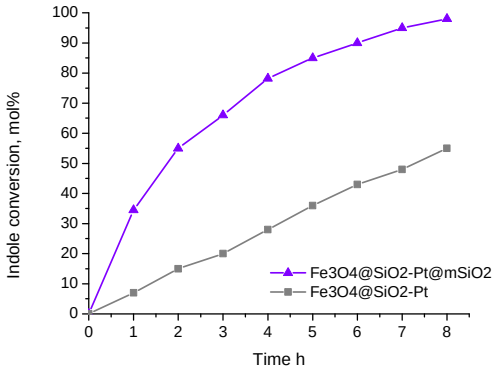

Figure 6. Indole conversion over the synthezised catalysts.

Figure 6 shows the conversion of indole as a function of time for the two synthesized catalysts. It is clearly observed that the catalyst with the mesoporous silica coating Fe_3O_4@SiO_2-Pt@mSiO_2 is much more active than the uncoated catalyst, reaching a complete conversion at 8 h of reaction, while Fe_3O_4@SiO_2-Pt only reaches 50% conversion. Figure 7 shows the molar fraction of the reaction system for both catalysts. In the case of Fe_3O_4@SiO_2-Pt (Figure 7.a), we can observe that indoline is formed first then OEA and that the appearance of EB and ECH is very slow. Contrary, for Fe_3O_4@SiO_2-Pt@mSiO_2 (Figure 7.b), the consumption of indole and the appearance of EB and especially ECH (the denitrogenated products) is very fast. The percentage of denitrogenated products (% HDN) was calculated and listed in Table 2. In the Table, the results were compared with those of a typical HDN catalyst NiMo/Al_2O_3 Criterion DN200 [7]. This catalyst was presulfided according to our previous reported results [7]. Catalyst

Fe_3O_4@SiO_2-Pt@mSiO_2 reached a higher % HDN value compared with the other two catalysts. A control reaction was carried out using Fe_3O_4@SiO_2 as a catalyst under the same conditions and no activity was obtained. This confirms the inactivity of the support.

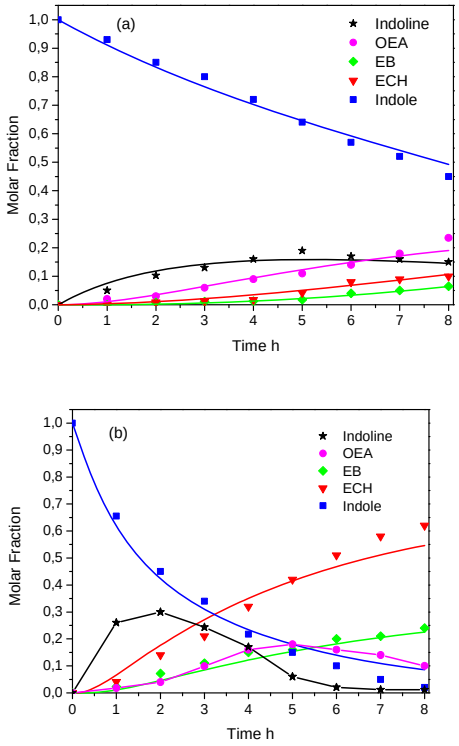

Figure 7. Molar fraction of indole and products in HDN reaction (a) Fe_3O_4@SiO_2-Pt; (b) Fe_3O_4@SiO_2-Pt@mSiO_2.

Table 2. Indole conversion and % HDN of the catalysts at reaction time of 8 h.

Catalysts	Indole Conv.	% HDN[1]
Fe_3O_4@SiO_2-Pt	55	30
Fe_3O_4@SiO_2-Pt@mSiO_2	98	88
NiMo/Al_2O_3 [11]	50	30

[1] %HDN= 100*(ECH+EB)/(ECH+EB+OEA+HIN)

The better activity of Fe_3O_4@SiO_2-Pt@mSiO_2 compared with NiMo/Al_2O_3 catalyst can be related to the high hydrogenating capacity of platinum in Fe_3O_4@SiO_2-Pt@mSiO_2. In the case of both core@shell structures is very clear that the difference in activity is due to the presence of the second porous shell and not to the dispersion of the platinum nanoparticles.

The large difference in activity has to be explained in relation to the presence of the mesoporous silica layer and in the greater surface area of Fe_3O_4@SiO_2-Pt@mSiO_2 compared with Fe_3O_4@SiO_2-Pt. Fe_3O_4@SiO_2-Pt@mSiO_2 possesses cylindrical channels perpendicular to the surface that correspond to the porosity of the material formed during the removal of the organic template. The synthesis of such coating was carried out using triethanolamine (TEA) as the basic catalyst, which leads to the surface of the SiO_2 generated remains negatively charged. The removal of CTAB was performed by ion exchange using ammonium nitrate in ethanol solution, this exchange by NH_4^+ cations allows them to adhere as counterions. The presence of these cations generates a slight surface acidity in the porous SiO_2 of the second coating [25]. Which greatly benefits HDN reactions as we demonstrated in previous work [7]. This is also evidenced in the greater obtaining of ECH with respect to EB with the Fe3O4@SiO2-Pt@mSiO2 catalyst, a behavior observed in catalysts with acidic characteristics [7]. For the other hand, in line with previous reported for heterogeneous core-shell catalysts with a porous coatings, the porosity and characteristics of the material of the second coating generate a confinement effect that could favor the adsorption of the reagent and the re-adsorption of the intermediates of the reaction, increasing the contact time between intermediates and the platinum active catalytic species. This behavior in core-shell catalysts with porous coatings was already observed by Jun Bao et al. [26].

3.3-Reutilization study

Catalyst reuse is important from an industrial point of view. In this case, the catalysts have been tested during four catalytic cycles. The samples were washed several times with a mixture of methanol and water previous to the reaction.

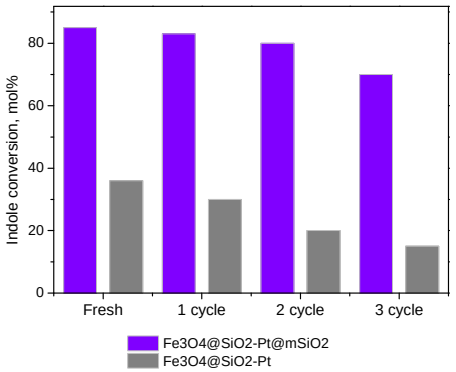

Figure 8. Reutilization study of the catalysts at 5 h of reaction time.

Figure 8 shows that the activity slightly decreases after the third recycle in the case of Fe_3O_4@SiO_2-Pt@mSiO_2, but the loss in activity is higher in the case of Fe_3O_4@SiO_2-Pt. The higher stability of Fe_3O_4@SiO_2-Pt@mSiO_2 could be due to the presence of the second porous silica coating that inhibits the loss of the metal charge and prevents sintering. The stabilization achieved after the second layer of silica allows the successive reuse of the catalyst. In addition, the magnetic characteristics of this catalyst facilitate the separation process, which is very important from the practical and economic perspective in any industrial process.

4. Conclusions

In this work, we studied the effect of a second porous SiO_2 shell in the activity and selectivity of the Fe_3O_4@SiO_2-Pt catalyst in the hydrodenitrogenation of indole. The core shell structures were applied for the first time in the indole HDN process. We found that the presence of a mesoporous SiO_2 coating dramatically increases the activity of the catalyst. The great difference in activity was explained in terms of a confinement effect of the intermediates products of the reaction in the second SiO_2 layer. This coating of slightly acidic character and with parallel mesochannels, favored the re-adsorption and transformation into denitrogenated products. The Fe_3O_4@SiO_2-Pt@mSiO_2 catalyst remained active after several catalytic cycles and its magnetic character allows its easy separation and recovery.

5. Acknowledgments

This research was funded by CONICYT-Chile grant Fondecyt 1170083.

6. References

[1]*Beltramone, A.R.; Resasco, D.E.; Alvarez, W.E.; Choudhary T.V., Ind. Eng. Chem. Res. 47(2008) 7161.*
[2]*Kishore Kumar, S.A.; John, M.; Pai, S.M.; Niwate, Y.; Newalkar, B.L., Fuel Process.Technol. 128(2014)303.*
[3]*Valles, V.A.; Ledesma, B.C.; Rivoira, L.P.; Cussa, J.; Anunziata, O.A.; Beltramone, A.R., Catal. Today 271(2016) 140.*
[4]*Egorova, M.; Prins, R.,. J. Catal. 224(2004)278.*
[5]*Nassreddine, S.; Massin, L.; Aouine, M.; Geantet, C.; Piccolo, L., J. Catal.278(2011) 253.*
[6]*Jongpatiwut, S.; Li, Z.; Resasco, D.E.; Alvarez, W.; Sughrue, E.; Dodwell, G., Appl.Catal. 262(2004)241.*
[7]*Ledesma, B.C.; Anunziata, O.A., Beltramone, A.R., Appl. Catal. B 192(2016)220.*
[8]*Ledesma, B.C.; Martínez, M.L.; Beltramone, A.R., Catal Today (2018) In press.*
[9]*Valles, V.A.; Ledesma, B.C.; Rivoira, L.P.; Cussa, J.; Anunziata, O.A.; Beltramone, A.R., Catal. Today 271(2016)140.*
[10]*Valles, V.A.; Ledesma, B.C.; Pecchi, G.A.; Anunziata, O.A.; Beltramone, A.R., Catal. Today 282(2017)111.*
[11]*Meynen, V.; Cool, P.; Vansant, E.F., Micropor. Mesopor. Mater 125(2009)170.*
[12]*Pachon, L.D.; Rothenberg, G., Appl. Organomet. Chem. 22(2008)288.*
[13]*Zhang, N.; Xu, Y.-J., Chem. Mater. 25(2013)1979.*
[14]*Zhang, Y.; Li, P., Mater. Des. 88(2015)1250.*
[15]*Majewski, A.J.; Wood, J.;Bujalski, W., Int. J. Hydrogen Energ. 38(2013)14531.*
[16]*Biradar, A.V.; Biradar, A.A.; Asefa, T., Langmuir 27(2011)14408.*
[17]*Shi, Y.-L.; Asefa, T., Langmuir 23(2007)9455.*
[18]*Scahtz, A.; Reiser, O.; Stark, W.J., Chem. Eur. J. 16(2010)8950.*
[19]*Long, Y.; Liang, K.; Niu, J.; Yuan, B.; Ma, J., Dalton T. 44(2015)8660.*
[20]*Yang, J.; Shen, D.; Wei, Y.; Li, W.; Zhang, F.; Kong, B.; Zhang, S.; Teng, W.; Fan, J.; Zhang, W.; Dou, S.; Zhao, D., Nano Res. 8(2015)2503.*
[21]*Zhang, W.; Shen, F.; Hong, R., Particuology 9(2011)179.*
[22]*Thommes, M.; Kaneko, K.; Neimark, A.V.; Olivier, J.; Rodriguez-Reinoso, F.; Rouquerol J.; Sing, K., Pure Appl. Chem. 87(2015)1051.*
[23]*Teng, Z.; Su, X.; Chen, G.; Tian, C.; Li, H.; Ai, L.; Lu, G., Colloid Surface A 402(2012)60.*
[24]*Zhang, L.; Ozkan, U.S., Stud. Surf. Sci. Catal. 101(1996)1223.*
[25]*Lanzafame, P.; Barbera, K.; Papanikolaou, G.; Perathoner, S.; Centi, G.; Migliori, M.; Catizzone, E.; Giordano, G., Catal. Today 304(2018)97.*
[26]*Bao, J.; He, J.; Zhang, Y.; Yoneyama, Y.; Tsubaki, N. Angew Chem Int ed. 47(2008)353.*